06

Strengthening polycrystalline ice with SiO_2 nanoparticles

© Yu.I. Golovin,[1,2] A.A. Samodurov,[1] V.V. Rodaev,[1] A.I. Tyurin,[1] D.Yu. Golovin,[1] S.S. Razlivalova,[1] V.M. Buznik[1,2]

[1] Tambov State University,
392036 Tambov, Russia
[2] Moscow State University,
119991 Moscow, Russia
e-mail: tyurinalexander@yandex.ru, yugolovin@yandex.ru

Received June 14, 2023
Revised July 26, 2023
Accepted July 27, 2023

The paper presents the results of ice strengthening by means of ultrafine silica nanoparticles introduced to distilled water prior to its crystallization. Stable SiO_2 particles suspensions with concentrations ranging from 0.003 to 5 wt.%. have been prepared, and nanoparticles size distribution and zeta potential have been monitored in them. Both values remain almost constant for a week. Concentration dependences of maximal stress, Young's modulus and inelastic deformation at and after reaching peak stress in uniaxial compression test have been studied. The highest rate of change with the particles concentration for these properties is between 0.01 and 1 wt.%. while beyond the above range the concentration sensitivity is much weaker. The strongest effect of silica concentration is on inelastic deformation, and the weakest effect is on Young's modulus. Concentration sensitivity of the properties has been estimated by the power index of the best fitted power function for each of the property. Dependence of strength upon average grain size, that diminishes sixfold with growing concentration, is well approximated by power function also, but with negative power index -1/2. Additive constant in this dependence is found to be much lower than the strength of large grain pure ice and is close to zero within experiment accuracy. Hence, the strength of studied polycrystalline ice and ice composites is limited by the nucleation and subsequent propagation of Griffiths cracks with characteristic length proportional to average size of ice grain.

Keywords: polycrystalline ice, mechanical properties, grain structure, ice composites, strengthening by nanoparticles, Hall–Petch and Griffiths relations.

DOI: 10.61011/TP.2023.10.57452.149-23

Introduction

The development of the Arctic, provided for by the state programs of the Russian Federation, needs the creation of road transport, industrial, household, social infrastructure. These long-term plans involve the construction of roads, runways, crossings, buildings and other structures for various purposes. All this requires large volumes of structural and construction materials, preferably from local, renewable, environmentally friendly sources of raw materials [1–3]. Ice, which is universally available in regions with a cold climate and does not require disposal at the end of its service life, could be one of the most promising building materials, but as such it has insufficient strength and high brittleness [4–8]. Therefore, many northern peoples, when erecting their winter dwellings such as igloo made of snow and ice have long reinforced them with moss, yagel and other plant components.

Excluding from consideration the methods of increasing the bearing capacity of ice during the construction of winter crossings, railways and highways by laying logs, branches, sleepers, beams, boards and other structural elements of meter scale on its surface, historically the first engineering approach to ice strengthening was its reinforcement with macro-additives of millimeter sizes. Most often, their role was played by cheap waste from the forestry industry (sawdust, shavings, wood chips) [9]. The most famous of such projects is Habbakuk (Habakkuk) [10] provided for the construction of large floating ocean islands in the Atlantic during World War II made of ice composites (IC) for using them as airfields. The addition of an optimal amount of sawdust to the frozen water (14 wt.%, which is about a third of the volume of the material) led to fourfold ice strengthening.

Over the course of more than a century of engineering developments aimed at strengthening ice with various micro- and macroscale additives, a number of approaches and technologies have been proposed for improving the load-bearing capacity of structures made of IC [11–15]. This made it possible to build from them quite large hydraulic structures and domed rooms with a diameter of tens of meters [16–18]. High-strength microfibers have been used in recent decades as reinforcing components in laboratory conditions — from microcellulose and basalt to Kevlar and nanostructured carbon [19–26]. However, the potential of approaches and methods for strengthening ice with macro- and micro-additives is very limited, which prevents their widespread use in the construction of large structures. In particular, these methods are not technological and require special measures to obtain stable suspensions. Hardening

with long („infinite“) microfibers requires technologies of their layer-by-layer laying and freezing, and employing fibrous matrice requires methods of combating trapped air bubbles. As a rule, all these methods of manufacturing IC increase the strength of ice by no more than 3−4 times, and only in rare, record cases — up to 5−6 times. They are not environmentally perfect and require special measures to dispose of the used modifiers after the end of the life cycle of the structure.

In the end, it became clear that it was impossible to achieve radical hardening of IC only with the help of micro- and macro-dimensional reinforcing additives. The main reason is that reinforcement with these components has almost no impact on the microstructure of the IC ice base, no matter what high-strength reinforcing elements are used. The strength of reinforced IC is limited by the imperfection of the crystal structure of ice and a large number of structural defects present in it. Apparently, for this reason, attempts to modify the molecular structure of ice using polymer additives (organofluorine compounds, polyvinyl alcohol) have also not been crowned with great success [27–31].

In this regard, it is important to note that, despite the relative weakness of the hydrogen bonds between the molecules H_2O [32], which determine the fundamental mechanical characteristics of ice, the theoretical limit of its strength σ_{th} is very high. As is known, the strength and Young's modulus E of ideal defect-free crystals, which is commonly called ideal or theoretical, are due to the properties of interatomic/molecular bonds and their density per unit area. Classical and quantum theories of solid state physics from the first principles, as well as computer modeling, give the value $\sigma_{th} \approx (0.07-0.1)E$ [33–35]. At the usual winter temperatures for the northern regions, only a few tens of degrees below the melting point of ice, for estimates we can take $\sigma_{th} \approx 0.05E_d \approx 500$ MPa, where $E_d \approx 10$ GPa — the dynamic value of the Young's modulus of pure ice [4,7,8]. The strength of natural ice, determined experimentally, is usually 2−3 orders of magnitude less than σ_{th} and amounts to 0.5−10 MPa [4,7]. This implies a large and not yet used reserve for strengthening ice and IC. The main reason for such a strong discrepancy between theoretical predictions and the experiment, obviously, is the presence of a wide range of structural defects in real ice and IC, primarily micro- and macro-cracks, air bubbles and other discontinuities. Therefore, the search for new ideas and approaches to realizing the existing potential of ice hardening is still relevant to this day.

This paper presents the results of a study of the addition of nanoparticles (NPs) to frozen water as one of the fields of such studies. In contrast to macro- and micro-dimensional components, NP addition can result in various changes in the microstructure of ice at smaller scale levels compared to simple reinforcement. However, the available information about the impact of NPs on the microstructure and properties of IC is very scarce. Data on the impact of NPs on the nucleation of crystallites in polycrystalline ice, on their growth, strength and thermophysical characteristics in industrial wastewater ponds and peat pits are provided in [36,37], while the data of studies in Yellow River in China are provided in [38]. Nano- and micro-sized particles can be present in concentrations up to 0.1 wt.% in the water of these reservoirs. The results of a study of the processes of inhibition of the growth of ice grains by cellulose nanoparticles during recrystallization are described in [39,40]. The results of several attempts to modify the microstructure and harden ice by deliberately introducing hydrophilic NPs into its structure are described in [41–44].

The given brief review of the literature demonstrates the following state of the problem of ice reinforcement. Though the entire range of modifiers characteristic sizes from molecular to macroscopic has been tested, no reproducible strengthening of IC by more than $4-5$ times has been achieved. Even though the theory allows for a further increase of strength, at least by another order of magnitude. However, almost unexplored „white spots“ remain on the map of methods for modifying the mechanical characteristics of ice. The least studied and promising area seems to be the intermediate interval between the molecular and microlevel, namely nano- and submicro-scale. This structural and hierarchical level can be mastered by introducing natural and synthetic, organic and inorganic NPs into the frozen water. This approach is consistent with one of two concepts well known in physical materials science. According to the first of them, it is necessary to reduce the concentration of defects, striving to obtain an ideal single crystal. This is unlikely to provide good prospects for ice-based materials, but, given its fragility, the elimination of micro- and macro-cracks, as well as other macro-heterogeneities that play the role of strong stress concentrators, can contribute to significant strengthening. In accordance with the second concept, significant strengthening of polycrystalline materials and approximation to theoretical strength can be achieved by increasing the concentration of small structural defects, bringing the material to an amorphous state in the limit.

We have shown in recent works [43,44] that the introduction of NPs into the ice structure makes it possible to increase the compressive strength by more than 6 times. The mechanisms of this strengthening are not yet completely clear, but the detected decrease of grain sizes with an increase of the impurity concentration and the size of the cracks associated with them definitely indicates the significant role of the latter in the formation of the mechanical characteristics of polycrystalline ice. Clarification of the role of NPs and grain boundary failure in the formation of mechanical characteristics of IC needs systematic studies. Unlike reinforcement with macroscopic components and microfibers, the introduction of NPs into the IC structure can have a diverse character, and the effects induced by their presence can have many different causes and micromechanisms. In particular, a consequence of the introduction of NPs into the ice may be a decrease of grain size and the resulting increase of yield strength, according

to the Hall–Petch ratio, and reducing the length of grain boundary cracks, blocking grain boundary cracks, dispersion hardening of grain volume and many other changes in the microstructure of ice.

The purpose of this work was to experimentally study the fundamental possibilities of hardening ice with hydrophilic NPs of silicon dioxide and to elucidate the micromechanisms of destruction under load that determine its uniaxial compression strength.

1. Materials and methods

IC samples were formed from hydrosols containing silicon dioxide NPs (Aldrich, USA). The size D stated by the manufacturer of these NPs was 10–20 nm. It was calculated based on the specific surface area of the NPs determined by the Brunauer–Emmett–Teller (BET). The initial 5 wt.% sol was first obtained by dispersing the corresponding NPs test charge in distilled water using ultrasonic liquid processor Vibra-Cell VCX 750 (Sonics & Materials, USA) to prepare hydrosols with a mass fraction of NPs ω in the range of 0.003–5 wt.%. The frequency of ultrasonic exposure was 20 kHz, and its power was limited to 100 W to prevent heating of the hydrosol. Then, hydrosols with a smaller mass fraction of NPs were prepared from the obtained 5% wt.% hydrosol by sampling and their sequential dilution with distilled water.

The NPs size distribution D in the prepared hydrosols was analyzed by dynamic light scattering (DLS) using analyzer Zetasizer Nano ZS (Malvern Instruments, UK), which was also used to determine the zeta potential of hydrosols. Fig. 1, *a* shows that there was a monomodal NPs distribution in size, the maximum of which was close to $D = 40$ nm. At the same time, the position of the distribution maximum did not depend on the mass fraction of NPs in the hydrosole. The insert of Fig. 1, *a* shows an image of a NPs obtained on a scanning electron microscope (SEM) Merlin (Carl Zeiss, Germany) with a field cathode. Analysis of SEM images showed that the NPs had a size of 25 ± 7 nm and a shape close to spherical. It should be noted that the DLS and SEM methods gave somewhat higher NPs size than that declared by the supplier, which may be due to both the specific parameters of the indirect method used by the manufacturer to determine the size of the NPs and the hygroscopicity of the silicon dioxide NPs.

The prepared hydrosols were stable over time regardless of the mass fraction of NPs in them. This is indicated by the stability of the distribution of the latter in size and the position of the distribution maximum over time (Fig. 1). After 6 days, both the median size of the NPs D_m and their zeta potential (Table. 1) remained unchanged within the statistical dispersion of the data. At the same time, for all hydrosols, the zeta potential exceeded 30 mV in absolute value at any given time, which is a well-known criterion for the stability of the colloidal system.

Distilled water and NPs hydrosols were poured into specially made fluoroplastic cuvettes with 48 cells isolated from each other in size $10 \times 10 \times 20$ mm for obtaining samples of pure ice and IC. The cuvettes had a thin bottom wall (~ 1 mm) and were located inside the freezer on a massive metal plate. After filling the samples, the cuvettes were insulated from the top and sides from the atmosphere of the freezer with a thick-walled foam screen. The samples were frozen at -10°C. Since the coefficient of thermal conductivity of ice is more than an order of magnitude higher than that of fluoroplast, this technical solution gave the heat flow a preferential direction „from top to bottom“ during crystallization, which reduced internal stresses and cracking in the sample.

The sizes of the samples were determined by several considerations. Their small volume ($2\,\text{cm}^3$) and the simultaneous production of 48 pieces under the same conditions allowed for a relatively small spread of data and representative statistics. At the same time, the transverse size of 10 mm exceeded the average grain size in any samples by more than an order of magnitude (see sec. 2), and at high concentrations of NPs — and by two orders of magnitude. This makes it possible to consider the influence of external dimensional effects on the experimental results negligible.

The grain structure of the obtained samples of pure ice and IC with different NPs content was studied using an Axio Observer.A1m optical microscope (Carl Zeiss, Germany) in reflected light. The microscope had an image capture and analysis system, as well as a removable thermal camera with adjustable forced cooling. Grain boundaries were visualized as a result of segregation of impurities in their vicinity and thermal etching.

The mechanical strength of the manufactured samples of pure ice and IC with different NPs content was studied by uniaxial compression using servo-hydraulic testing machine MTS 870 Landmark (MTS, USA). A temperature of -10°C was maintained inside the climate chamber of the machine by purging it with liquid nitrogen vapors. The rate of relative deformation in all experiments was $4 \cdot 10^{-3}\,\text{s}^{-1}$. Uniaxial compression tests were performed on at least eight samples at each NPs concentration. A total of 142 samples were tested.

2. Results

Fig. 2, *a, c, e, g* shows a typical granular microstructure of prepared samples of pure ice and IC with different NPs content. It can be seen from the figures that an increase of the NPs content leads to a decrease of grain sizes d, averaged for each grain in two mutually perpendicular directions. The analysis of grain size distribution (Fig. 2, *b, d, f, h*) showed that in pure ice, the value of d varies in the range from 100 to 1200 μm with a median value $d_m = 500 \pm 50\,\mu$m. With an increase of ω, a narrowing of the range of values of d and a shift of d_m towards

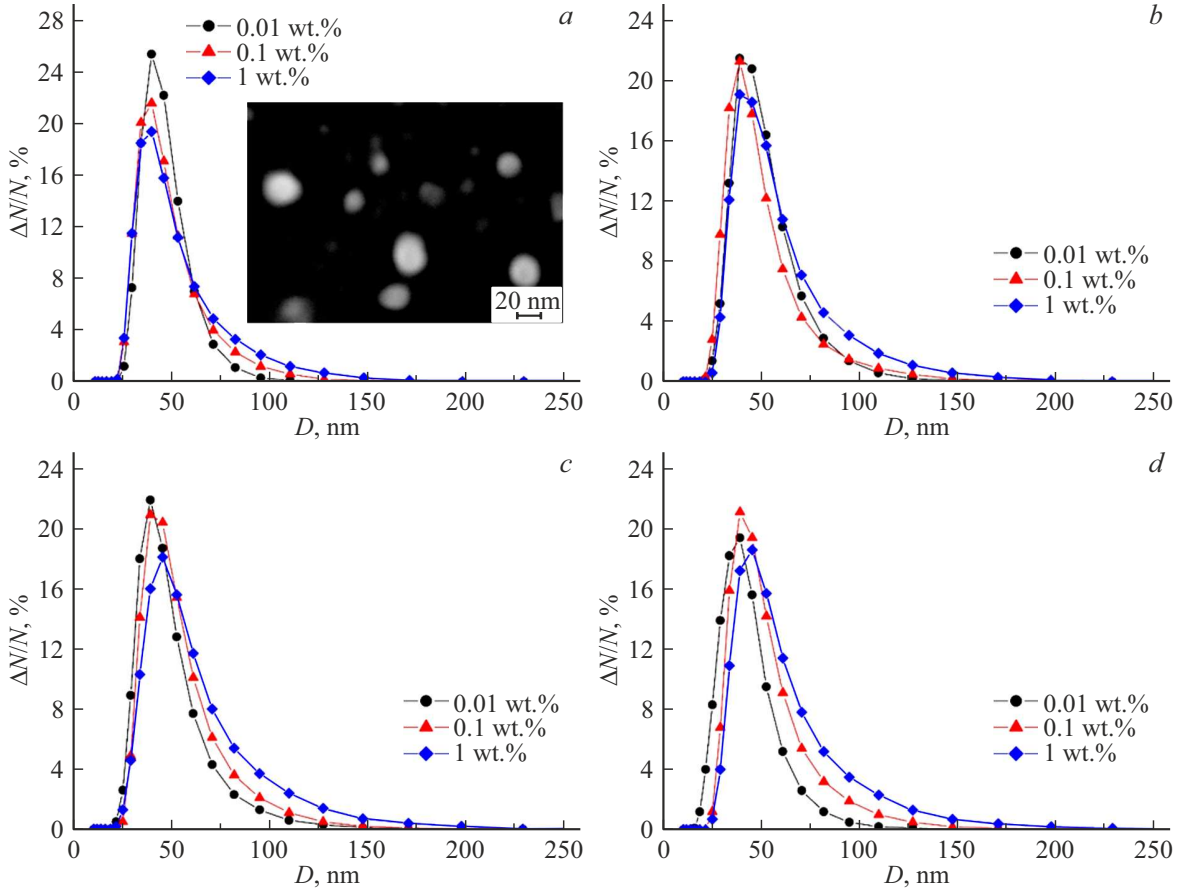

Figure 1. Dynamics of changes in the distribution of NPs by size D in suspensions with different contents ω for 6 days: freshly prepared suspensions (a), after one day (b), after three days (c), after six days (d). The insert of Fig. 1, a shows a SEM image of NPs.

Table 1. Zeta potential of suspensions with different NPs content after different time from the moment of their preparation

Time, days	0			1			3			6		
Mass fraction NPs-SiO_2, wt.%	0.01	0.1	1	0.01	0.1	1	0.01	0.1	1	0.01	0.1	1
Zeta remove the last hyphen, mV	-39 ± 5	-40 ± 5	-38 ± 4	-41 ± 4	-38 ± 4	-37 ± 5	-38 ± 6	-39 ± 5	-35 ± 5	-38 ± 3	-37 ± 4	-34 ± 6
Average value of zeta–potential, mV	-39 ± 5			-39 ± 4			-37 ± 5			-36 ± 4		

smaller values was observed. So, while at $\omega = 0.003$ wt.% $d_m = 450 \pm 50\,\mu$m, at $\omega = 5$ wt.% $d_m = 95 \pm 5\,\mu$m.

Figure 3 shows typical loading diagrams for samples of pure ice and IC in coordinates $\sigma - \varepsilon$, where σ — engineering stresses of uniaxial compression, and ε — relative deformation. Several characteristic sections can be distinguished on the curves $\sigma - \varepsilon$. The initial section of the loading diagram with a small slope, resulting from small irregularities of the ends of the sample, was not taken into account in the future and was excluded when analyzing the diagram. Further, the deformation linearly increased with an increase of load, which was observed in pure ice and IC with low NPs content of $\omega < 0.01$ wt.% up to brittle failure of the material without irreversible deformation recorded

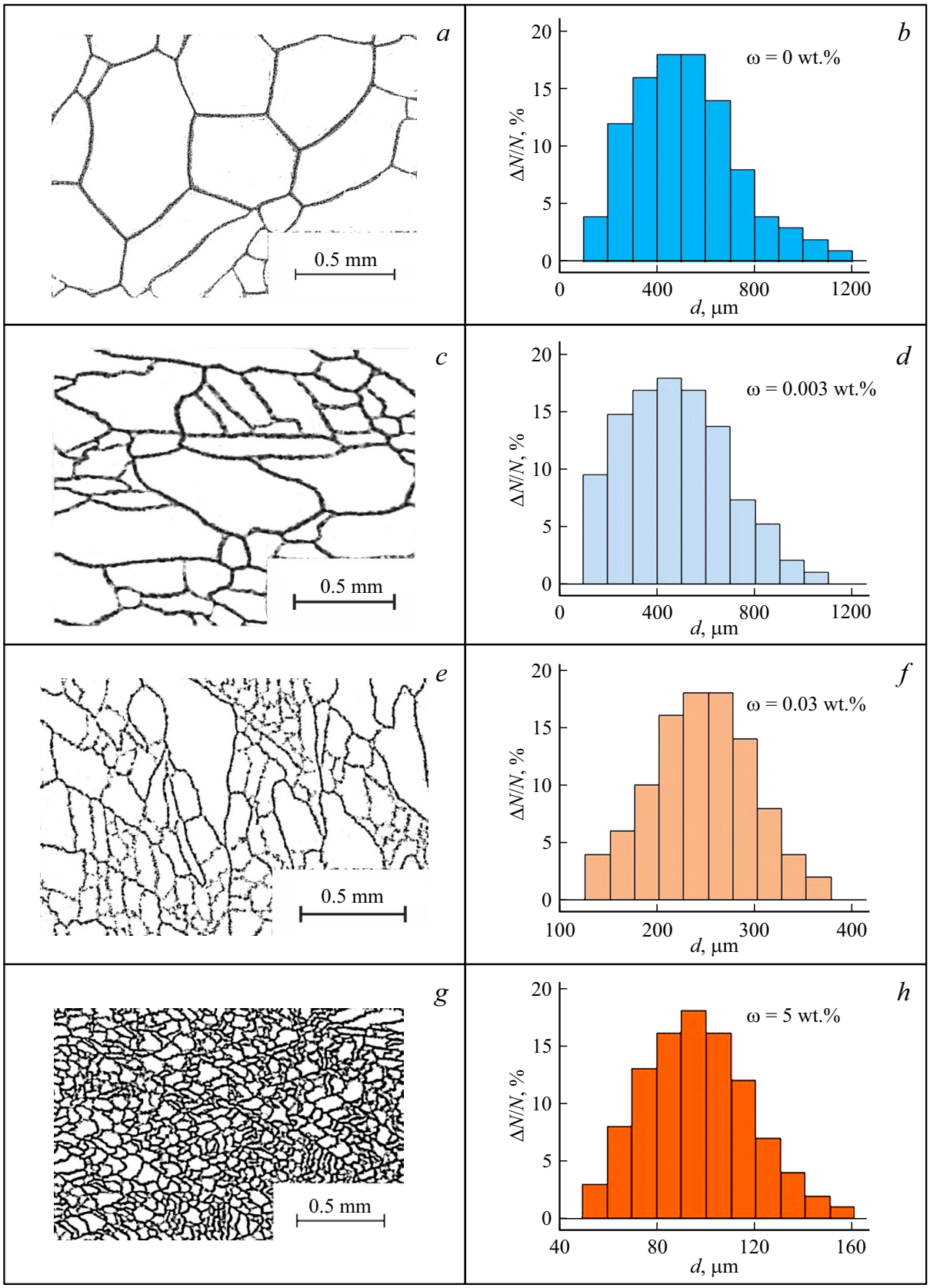

Figure 2. Microstructure (*a, c, e, g*) and grain size distribution (*b, d, f, h*) of pure ice and IC with different NPs content ω. Pure ice — (*a, b*); IC ($\omega = 0.003$ wt.%) — (*c, d*); IC ($\omega = 0.03$ wt.%) — (*e, f*); IC ($\omega = 5$ wt.%) — (*g, h*).

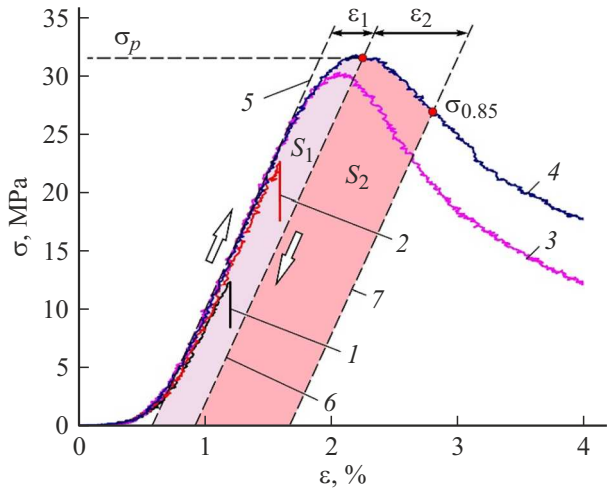

Figure 3. Typical deformation curves $\sigma-\varepsilon$ for pure ice —*1*, IC ($\omega = 0.3\%$) — *2*, IC ($\omega = 3\%$) — *3* and IC ($\omega = 5\%$) — *4*. The point $\sigma_{0.85}$ indicates a stress equal to 85% of σ_p. The areas S_1 and S_2 bounded by a curve and dashed lines *5*–*6* and *6*–*7* are proportional to the specific work A_1 and A_2, spent on deforming samples to reach σ_p and then to $\sigma_{0.85}$, respectively. The corresponding relative inelastic deformations are designated as ε_1 and ε_2.

by the testing machine. The slope of the linear section (along the line *5*) was taken as the conditional Young's modulus E of the material. Irreversible deformation of ε_1 before destruction and confidently recorded hardening compared to pure ice occurred at $\omega > 0.01$ wt.%. The stress after reaching the maximum σ_p did not jump to zero at $\omega > 3$ wt.%, but gradually decreased. At the same time, the sample maintained its integrity. As a result, a long section of quasi-plastic flow (> 10% deformation) were observed in these IC, which qualitatively distinguished these samples from samples with a smaller ω, which demonstrated quasi-brittle destruction immediately after reaching the maximum stress. Below by the strength of pure ice and IC, we will mean this ultimate stress σ_p sustained by the material during testing. The strengthening of the ice by NPs will be characterized by the coefficient $k = \sigma_p/\sigma_p^*$, where σ_p^* — the maximum stress sustained by pure ice. Accordingly, for pure ice $k = 1$. The stress $\sigma_{0.85}$, which is 85% of σ_p, is often taken as a measure of the load-bearing capacity of ICs that show viscoelastic falure behavior [45].

Concentration dependences of σ_p, E, ε_1, ε_2, A_1 and A_2 are shown in Figures 4 and 5. The symbols A_1 and A_2 denote specific work (proportional to the areas S_1 and S_2, marked in Fig. 3), spent on deforming samples to reach σ_p and further to $\sigma_{0.85}$, respectively. The corresponding relative inelastic deformations are denoted as ε_1 and ε_2 (see Fig. 3).

In general, the considered mechanical characteristics of IC increased with an increase of ω for all dependences. However, the sensitivity of individual characteristics to the change of ω was different. The dependence $\sigma_p(\omega)$ was characterized by a slowdown in growth at $\omega > 1$ wt.%, then it reached saturation (Fig. 4, *a*). The coefficient k reached 2.5 at $\omega = 5$ wt.%. The dependence $E(\omega)$ was expressed much weaker than $\sigma_p(\omega)$ (Fig. 4, *b*). At maximum, the increase of E in IC (at $\omega = 1$ wt.%) did not exceed 25% compared to pure ice, and with a further increase of the NPs content in IC, their Young's modulus even decreased slightly.

It is important to note that at $\omega > 1-3$ wt.%, the growth of mechanical characteristics was saturated, so from a practical point of view, a further increase of ω does not make much sense. As already noted above, signs of irreversible deformation began to appear in IC at $\omega > 0.01$ wt.% as distinguished from pure ice, which was expressed in the deviation of the dependence of $\sigma-\varepsilon$ from a straight line *5*. This occurred at stresses exceeding σ_p^* for pure ice (Fig. 3).

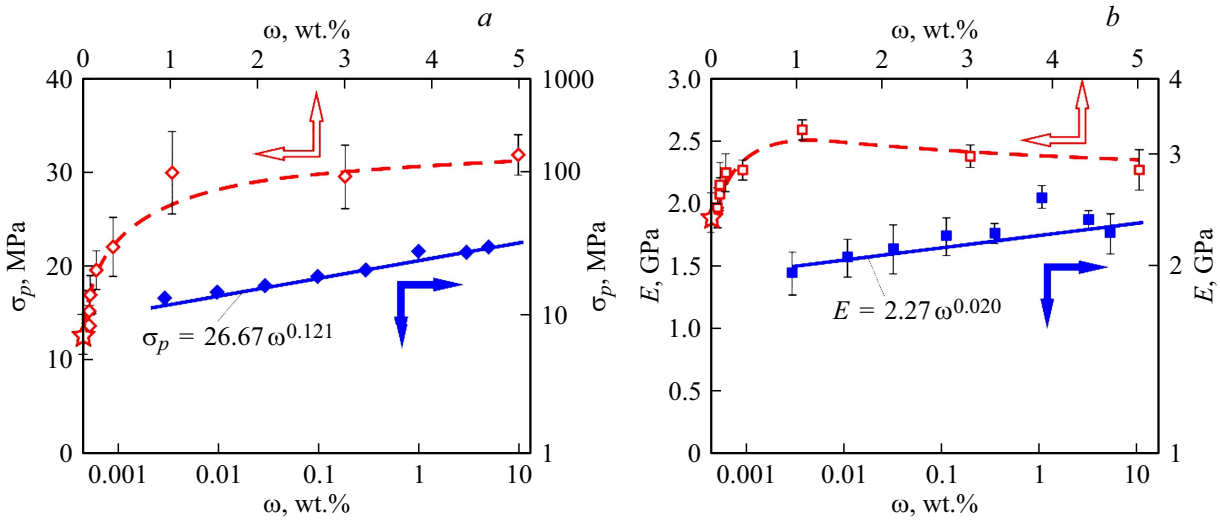

Figure 4. Dependence of peak stress σ_p (*a*) and Young's modulus E (*b*) on the mass fraction of the NPs ω in linear (empty red icons (in online version)) and logarithmic (solid blue icons (in online version)) coordinates. The mechanical characteristics of pure ice are marked with an asterisk.

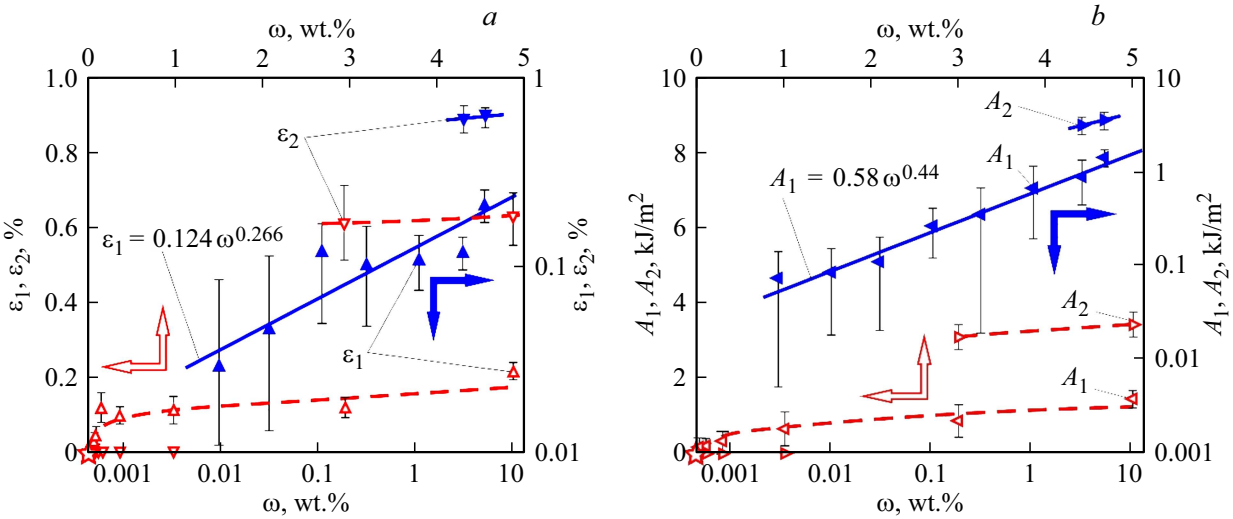

Figure 5. The dependences of relative inelastic deformations ε_1 and ε_2 (a) and specific work A_1 and A_2 (b) on the mass fraction of the NPs ω in linear (empty red icons (in online version)) and logarithmic (solid blue icons (in online version)) coordinates. The parameters of pure ice are marked with an asterisk.

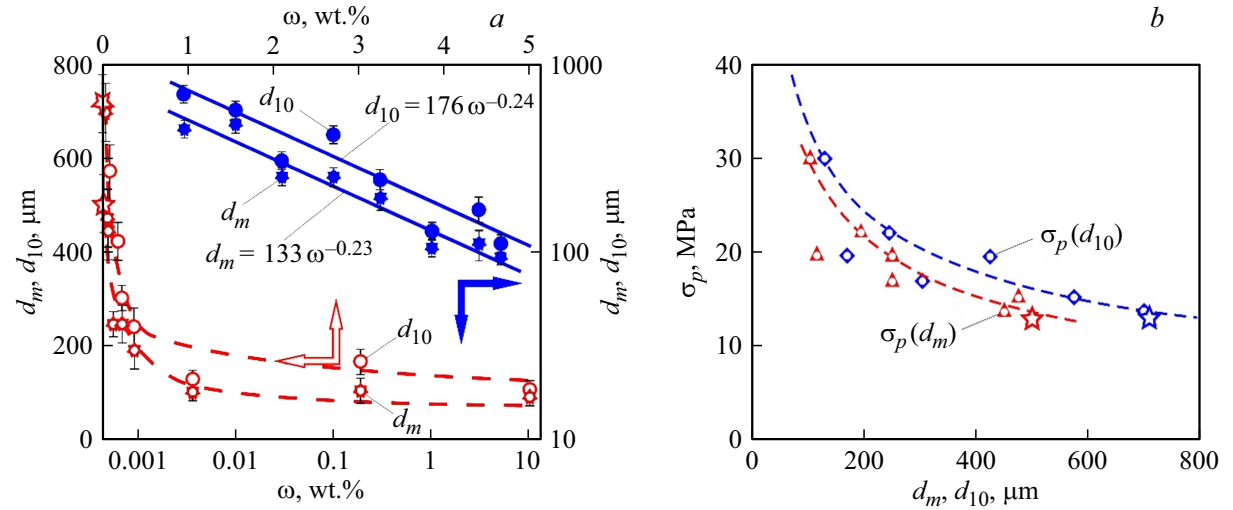

Figure 6. Dependence of grain size d_m and d_{10} of pure ice (asterisk) and IC with NPs additives on their mass fraction ω in linear (empty red icons (in online version)) and logarithmic (solid blue icons (in online version)) coordinates (a). Dependence of peak stress σ_p of pure ice and IC with NPs on grain size d_m and d_{10} (b).

The magnitude of this irreversible deformation ε_1 increased with an increase of ω (Fig. 5, a). The work A_1 (Fig. 5, b) spent on deformation before reaching peak stress also grew σ_p proportionately to ε_1 and σ_p. A brittle-viscous transition took place at $\omega = 1-3$ wt.%. The energy of complete fracture increased by more than an order of magnitude and it exceeded A_1 by 2.5–3 times when the stress changed to $\sigma_{0.85}$ (Fig. 5).

Grain sizes and the strength of grain boundaries can play an important role in the mechanical behavior of any polycrystalline materials. Similar effects are described in ice in [46]. It follows from dependence $d_m(\omega)$ shown in Fig. 6 that the introduction of NPs into the ice at a concentration of 1–2 wt.% leads to a decrease of d_m up to 6 times compared to pure ice. With a further increase of ω, saturation of the dependence of $d_m(\omega)$ was observed, as in the case of the mechanical characteristics of IC discussed above, which indicates a strong relationship between the latter and the grain size. A similar dependence was observed for the grain size d_{10}, which characterizes 10% of grains with maximum sizes in the distribution (Fig. 6).

Thus, the analysis of experimental data showed that the strongest impact on the studied mechanical characteristics and grain structure of IC is exerted by NPs at ω in the range from 0.01 to 1–2 wt.%. Rearrangement of experimental data in the specified range of NPs concentrations in double logarithmic coordinates showed that the considered mechanical characteristics of IC demonstrate a linear relationship

Table 2. Slope n and correlation coefficient r for the dependencies between logarithms different physical and mechanical characteristics of IC and logarithm ω

d_m		σ_p		E		ε_1		A_1	
n	r	n	r	n	r	n	r	n	r
-0.23 ± 0.03	-0.930	0.12 ± 0.01	0.987	0.02 ± 0.01	0.725	0.27 ± 0.05	0.923	0.44 ± 0.08	0.968

with the NPs concentration with high correlation coefficients r (Table 2). For the Young's modulus, which had a very weak dependence on ω, the value of r was significantly lower than for the other mechanical characteristics of IC. A good alignment of mechanical characteristics and grain size data in double logarithmic coordinates allows talking about the power nature of their dependencies on ω (Fig. 4–6), which makes it possible to quantify and then compare the strength of the influence of the NPs concentration on various characteristics of the IC in dimensionless magnitude n.

3. Discussion

As follows from Fig. 6, a more than sixfold decrease of the most probable grain size was observed with an increase of IC concentration. Therefore, first of all, we will discuss the mechanisms of IC strengthening associated with this effect. The observed decrease of grain size is obviously attributable to an increase of the number of centers of heterogeneous crystallite nucleation in the sample volume with the growth of ω. However, not every NPs manages to become the center of nucleation. Simple estimates show that, depending on the impurity concentration, the average grain size exceeds the average distance between the NPs with a diameter of 40 nm by 2–3 orders of magnitude. The majority of the NPs is pushed back by the crystallization front to the grain boundaries and changes their structure.

Grain boundaries, triple junctions, texture are the most important components of the microstructure of any polycrystalline materials, including ice and IC. Grain boundaries are a source and drain for dislocations, stress concentrators and, consequently, a place of facilitated crack generation and grain boundary sliding [46]. As is known, the strengthening effect of these factors can be described by the universal empirical Hall–Petch ratio (1) [6–8,46]:

$$\sigma_p = a + G/d_m^n, \qquad (1)$$

where a, G and $n \approx 0.5$ can be considered as constants of the material in the first approximation.

The probability of multiplication and movement of dislocations in the planes of basic sliding obeys similar ratios, which leads to dispersion hardening. Grain boundaries can be an effective barrier and block the breakthrough of dislocation accumulation from one grain to another. NPs can both inhibit grain boundary sliding and embrittle grain boundaries. n may differ slightly in the above processes from 0.5 and lie in the range from 0.3 to 0.8 [47].

The low fracture viscosity of pure ice (it is about an order of magnitude less than that of silicate glasses) causes the easy nucleation of microcracks in it. As a rule, the strength of grain boundaries in ice and IC with low NPs concentration is significantly lower than the strength of the grains themselves, and local stresses are higher, so cracks are formed mainly along the grain boundaries. Their most likely length coincides with the grain size, so a reduction of d_m (and, apparently, to an even greater extent d_{10}) can lead to strengthening in accordance with the Griffiths ratio [8]:

$$\sigma_p = B/d_m^{1/2}, \qquad (2)$$

where $B = (2E\gamma)^{1/2}$, and γ — effective surface energy.

The dependences $\sigma_p = f(d_m)$ were found and constructed in different coordinates to make a choice between the above-mentioned possibilities of strengthening using NPs, which are characterized by similar patterns (Fig. 7). It should be expected that the dependence of stresses on grain sizes will also be power-mode since the experimental concentration dependences of both σ_p and d_m demonstrate of a power-mode. Nonlinear regression of the experimental dependence $\sigma_p(d_m)$ by power functions by methods described in [48] for IC containing SiO2 NPs yields exponent close to -0.5 with the error of about 10% as shown in [43,44].

A linear regression in coordinates $\sigma_p - d_m^{-1/2}$ was used in this study on this basis. The values of the additive term $a = -1.7 \pm 2.2$ MPa (1) and the dimensionless correlation coefficient $r = 0.956$ are obtained as a result. Taking into account the high values of the correlation coefficient and the fact that the experimental values σ_p vary in the range $\sim 10-30$ MPa, it can be considered that the value of the additive term is equal to zero within the accuracy of the experiment and the dependence $\sigma_p(d_m)$ obeys the law $\sigma_p = Bd_m^{-1/2}$ (2). A direct linear regression of data in double logarithmic coordinates also leads to a degree of $n = -0.464$ close to $-1/2$. Experimental dependences $\sigma_p(d_m)$ and $\sigma_p(d_{10})$ are shown on fig. 7 in linearizing $\sigma_p - d_m^{-1/2}$ and double logarithmic coordinates along with the results of linear regression of data in these coordinates.

Thus, according to the results of processing the experimental data obtained, the mechanism of deformation and destruction of IC is most likely due to the development of cracks between grains formed from defects, the initial characteristic size of which linearly depends on the size of the grains.

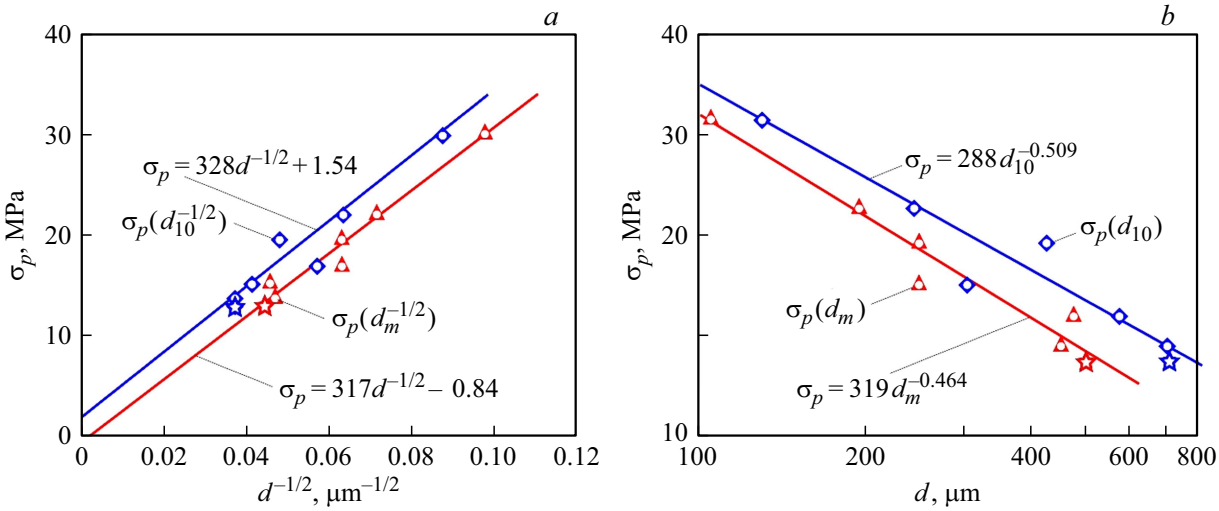

Figure 7. The dependence of the peak stress σ_p IC with NPs on d_m and d_{10}, approximated by the Griffiths ratio, depicted in the linearizing coordinates $d^{-1/2}$ (*a*), and the Hall–Petch ratio, depicted in logarithmic coordinates (*b*).

The appearance and growth of irreversible deformation in the IC before reaching maximum stresses and after it means a transition from brittle fracture, typical for pure ice and IC with a low impurity content, to viscoelastic at higher ω. The nature of this transition can be very diverse and needs clarification.

Conclusion

The regularities of strengthening of freshwater ice by highly dispersed silicon dioxide nanoparticles in free uniaxial compression test were identified. It is shown that the greatest increase of mechanical properties (compressive strength, Young's modulus, inelastic deformation before and after reaching peak load) occurs in the range of changes in the mass fraction of NPs ω from 0.01 to 1 wt.%. With a further increase of the NPs content to 5 wt.%, the mechanical characteristics of IC increased slightly, or did not change at all, reaching saturation at $\omega = 3-5$ wt.%.

The introduction of NPs, which are additional nuclei of heterogeneous crystallization leads to a decrease of the grain size of polycrystalline ice, the stronger the higher the impurity concentration. At maximum at $\omega = 5$ wt.%, the effect of grain size reduction reached more than sixfold in comparison with pure ice. The experimental dependence of strength on the median grain size was similar to Hall–Petch or Griffith law. However, the correlation statistical analysis of the data showed that the additive constant in the Hall–Petch ratio is close to zero or, at least, an order of magnitude less than the lowest values of peak stresses during the uniaxial compression test. Hence, the prevailing factor determining the strength of polycrystalline ice was the size of intergranular Griffith cracks, linearly related to the grain diameter and numerically almost equal to it. This result gives an indication of the directions for further studies and development of methods for strengthening IC by preventing the appearance or blocking the growth of these cracks. The results obtained provide a new vector for further research and development of methods for hardening IC by modifying the microstructure of ice by introducing ultrafine NPs.

Methods of modification of the structure and mechanical properties of ice and IC using NPs can be developed and applied both independently and in combination with other known methods. These methods can include chemical modification of the matrix with polymer additives, reinforcement with microfibers of natural and synthetic origin, heat treatment, mechanical „training " with constant and oscillating stresses, thermomechanical processing and other technologies.

Funding

This study was supported by the Russian Science Foundation (grant 22-19-00577). The results were obtained using the equipment of the Shared Use Center of Scientific Equipment at Derzhavin TSU.

Conflict of interest

The authors declare that they have no conflict of interest.

References

[1] A.A. Dynkin, V.A. Vernikovsky, N.L. Dobretsov, A.E. Kontorovich, N.S. Bortnikov, M.V. Flint, G.A. Romanenko, A.G. Litvak, V.M. Kotlyakov, A.A. Velichko, T.Ya. Khabrieva, A.Ya. Kapustin, I.I. Mokhov, V.P. Melnikov, V.A. Tishkov, N.I. Novikova, E.A. Pivneva, V.V. Stepanov, L.I. Aftanas, M.I. Voevoda, V.P. Puzyrev, L.M. Zeleny, A.N. Chilingarov, G.S. Kazanin, G.I. Ivanov, E.S. Makarov, V.I. Pavlenko, V.V. Rozhnov, L.I. Lobkovsky, A.I. Khanchuk, V.V. Kolomeichenko, R.V. Goldstein, Y.V. Tsvetkov, G.A. Month,

R.I. Nigmatulin, V.A. Rubakov, L.D. Fadeev, V.E. Fortov, N.G. Yakovlev, M.Yu. Ovchinnikov, Ya.V. Mashtakov, S.S. Tkachev, I.B. Petrov, V.G. Gitis, A.P. Vainshok, A.B. Derendyaev, V.V. Klimenko, V.M. Buznik, E.N. Kablov, A.A. Koshurina, V.V. Rozhkov, G.G. Matishov, A.I. Tatarkin, V.A. Kryukov, P.Ya. Baklanov, A.V. Moshkov, M.T. Romanov, N.A. Goryachev, N.V. Galtseva, V.E. Glotov, P.S. Minyuk, A.V. Lozhkin, A.S. Astakhov, A.L. Maksimov, Ya.N. Semenikhin, E.M. Novoseltsev, V.A. Stonik, V.V. Mikhailov, N.P. Pokhilenko, V.V. Sagaradze, N.V. Kataeva, S.Yu. Mushnikova, G.Yu. Kalinin, V.A. Malyshevsky, O.A. Kharkiv, A.M. Askhabov, S.K. Kuznetsov, I.N. Burtsev, V.D. Bogdanov, S.V.Kornilkov, V.L. Yakovlev, V.D. Kantemirov. *Nauchno-tekhnicheskie problemy osvoeniya Arktiki* (Nauka, M., 2015) (in Russian).

[2] V.M. Buznik, N.P. Burkovskaya, I.V. Zibareva, N.P. Andreeva, K.G. Bogolitsyn, L.B. Boynovich, S.Yu. Bratskaya, N.K. Vasiliev, S.V. Gnedenkov, G.Yu. Goncharova, V.P. Danilov, A.G. Dedov, A.M. Egorin, A.M. Emelianenko, L.N. Efimova, V.V. Zheleznov, A.V. Zhurko, E.A. Ivanova, V.K. Ivanov, O.I. Koifman, D.F. Kondakov, T.A. Kochina, L.N. Krasilnikova, V.I. Lozinsky, A.S. Lyadov, A.L. Maksimov, D.V. Mashtalyar, A.I. Nikolaev, E.A. Nikolaev, A.P. Petrova, S.N. Popov, N.P. Prophokova, A.A. Sagomonova, M.A. Sanjieva, M.D. Sokolova, Ya.A. Timantsev, S.A. Khatipov, I.N. Tsvetkova, R.N. Cherepanin, O.A. Shilova. *Arkticheskoe materialovedenie: sostoyanie i razvitie* (Gubkin Russian State University of Oil and Gas, Moscow, 2021) (in Russian).

[3] V.M. Buznik, E.N. Kablov. Herald Russ. Academy Sci., **87** (5), 397 (2017). DOI: 10.1134/S101933161705001X

[4] L.U. Arenson, W. Colgan, H.P. Marshall. In: *Snow and Ice-Related Hazards, Risks, and Disasters*, Eds. W. Haeberli, C. Whiteman (Elsevier Inc., 2021), p. 35. DOI: 10.1016/B978-0-12-817129-5.00007-X

[5] J.J. Petrovich. J. Mater. Sci., **38**, 1 (2003). DOI: 10.1023/A:1021134128038

[6] E.M. Schulson. J. Minerals, Metals, Mater. Society, **51** (2), 21 (1999). DOI: s11837-999-0206-4-1

[7] G.W. Timco, W.F. Weeks. Cold Regions Sci. Technol., **60**, 107 (2010). DOI: 10.1016/j.coldregions.2009.10.003

[8] E.M. Schulson, P. Duval. *Creep and Fracture of Ice* (Cambridge: Cambridge University Press, 2009)

[9] A. Pronk, N. Vasiliev, J. Belis. Structures and Architecture, **7**, 339 (2016). DOI: 10.1201/b20891-45

[10] L.W. Gold. Interdisciplinary Sci. Rev., **29** (4), 373 (2004). DOI: 10.1179/030801804225018783

[11] N.K. Vasiliev, A.D.C. Pronk, I.N. Shatalina, F.H.M.E. Janssen, R.W.G. Houben. Cold Regions Sci. Technol., **115**, 56 (2015). DOI: 10.1016/j.coldregions.2015.03.006

[12] J.H. Li, Z. Wei, C. Wu. Mater. Design, **67**, 464 (2015). DOI: 10.1016/j.matdes.2014.10.040

[13] N.K. Vasiliev, A.A. Ivanov, I.N. Shatalina. Vestn. Novosib. Gos. Univ., Ser. Mat. Mekh. Inform., **13** (3), 31 (2013).

[14] O.V. Yakimenko, V.V. Sirotyuk. *Usilenie ledovyh pereprav geosinteticheskimi materialami* (SibADI, Omsk, 2015) (in Russian).

[15] N.K. Vasiliev, A.D.S. Pronk. Izv. Veros. NII gidrotekhniki im. B.E. Vedeneeva, **277**, 35 (2015) (in Russian).

[16] A. Pronk, M. Mistur, Q. Li, X. Liu, R. Blok, R. Liu, Y. Wu, P. Luo, Y. Dong. Structures, **18**, 117 (2019). DOI: 10.1016/j.istruc.2019.01.020

[17] Y. Wu, X. Liu, B. Chen, Q. Li, P. Luo, A. Pronk. Automation in Construction, **106** (12), 102862 (2019). DOI: 10.1016/j.autcon.2019.102862

[18] A.S. Syromyatnikova, L.K. Fedorova. Arctic Ecology and Economy, **12** (2), 281 (2022). DOI: 10.25283/2223-4594-2022-2-281-287

[19] N.K. Vasiliev. Cold Regions Sci. Technol., **21**, 195 (1993). DOI: 10.1016/0165-232X(93)90007-U

[20] A.S. Syromyatnikova, A.M. Bol'shakov, A.V. Alekseeva. IOP Conf. Series: Earth and Environmental Sci., **459**, 062119 (2020). DOI: 10.1088/1755-1315/459/6/062119

[21] V.M. Buznik, G.Yu. Goncharova, G.A. Nuzhnyi, N.D. Razomasov, R.N. Cherepanin. Inorganic Mater.: Appl. Res., **10**, 786 (2019). DOI: 10.1134/S2075113319040087

[22] P.J.S. Cruz, J. Belis. In: *Structures and Architecture*, eds. P.J.S. Cruz (Taylor & Francis Group: London, 2016), p. 348. DOI: 10.1201/b20891-46

[23] X. Lou, Y. Wu. Cold Regions Sci. Technol., **192**, 103381 (2021). DOI: 10.1016/j.coldregions.2021.103381

[24] E.V. Morozov, A.S. Voronin, S.V. Kniga, V.M. Buznik. Inorganic Mater.: Appl. Res., **13**, 217 (2022). DOI: 10.1134/S2075113322010270

[25] V.M. Buznik, G.Y. Goncharova, D.V. Grinevich, G.A. Nuzhny, N.D. Razomasov, D.O. Turalin. Cold Regions Sci. Technol., **196**, 103490 (2022). DOI: 10.1016/j.coldregions.2022.103490

[26] G.A. Nuzhnyi, V.M. Buznik, R.N. Cherepanin, N.D. Razomasov, G.Y. Goncharova. InorganicMater.: Appl. Res., **12** (1), 236 (2021). DOI: 10.1134/S2075113321010287

[27] Q. Lu, Y. Ma, W. Yang. Acta Polym. Sin., **009** (11), 1166 (2009). DOI: 10.3724/SP.J.1105.2009.01166

[28] G.Y. Goncharova, N.D. Razomasov, G.V. Borshchev, V.M. Buznik. Theor Found Chem. Eng., **55**, 1045 (2021). DOI: 10.1134/S0040579521050055

[29] G.Y. Goncharova, R.O. Stepanov, T.S. Razomasova, I.A. Korolev, D.O. Turalin, Yu.A. Kulagin, Yu.G. Parshikov. Russ. J. Gen. Chem., **91** (Suppl. 1), S34 (2021). DOI: 10.1134/S1070363221130351

[30] J. Xie, M.-L. Yan, J.-B. Yan. Cold Reg Sci Technol., **206** (4), 103751 (2022). DOI: 10.1016/j.coldregions.2022.103751

[31] M.-L. Yan, X. Jian, J.-B. Yan. J. Build. Eng., **65**, 105751 (2023). DOI: 10.1016/j.jobe.2022.105757

[32] V.F. Petrenko, R.W. Whitworth. *Physics of Ice* (Oxford University Press, 2002)

[33] H.T. Courtney. *Mechanical Behavior of Materials* (Waveland Press, 2005)

[34] C.-T. Sun, Z. Jin. *Fracture Mechanics* (Waltham, MA: Academic Press, 2011)

[35] J. Pokluda, M. Černý, P. Šandera, M. Šob. J. Computer-Aided Mater. Des., *11*, 1 (2004). DOI: 10.1007/s10820-004-4567-2

[36] W. Gao, D.W. Smith, D.C. Sego. Cold Reg. Sci. Technol., **29** (2), 121 (1999). DOI: 10.1016/S0165-232X(99)00019-1

[37] M. John, M. Suominen, Otto-V. Sormunen, M. Hasan, E. Kurvinen, P. Kujala, A. Mikkola, M. Louhi- Kultanen. Water Res., **145**, 418 (2018). DOI: 10.1016/j.watres.2018.08.063

[38] Y. Deng, L. Zongkun, L. Zhijun, J. Wang. Cold Regions Sci. Technol., **168**, 102896 (2019). DOI: 10.1016/j.coldregions.2019.102896

[39] T. Li, Y. Zhao, Q. Zhong, T. Wu. Biomacromolecules, **20**, 1667 (2019). DOI: 10.1021/acs.biomac.9b00027
[40] T. Li, Q. Zhong, B. Zhao, S. Lenaghan, S. Wang, T. Wu. Carbohydrate Polymers, **234**, 115863 (2020). DOI: 10.1016/j.carbpol.2020.115863
[41] M. Yasui, E.M. Schulson, C.E. Renshaw. J. Geophys. Res. Solid Earth, **122**, 6014 (2017). DOI: 10.1002/2017JB014029
[42] Y. Hou, X. Su, M. Dou, C. Lu, J. Liu, W. Rao. Nano Lett., **21** (1), 00514 (2021). DOI: 10.1021/acs.nanolett.1c00514
[43] Yu.I. Golovin, A.A. Samodurov, V.V. Rodaev, A.I. Tyurin, D.Yu. Golovin, S.S. Razlivalova, V.M. Buznik. Tech. Phys. Lett. (2023) (in press).
[44] V.M. Buznik, Yu.I. Golovin, A.A. Samodurov, V.V. Rodaev, S.S. Razlivalova, A.I. Tyurin, D.Yu. Golovin. Inorganic Mater.: Appl. Res., 2023 (in press).
[45] J. Xie, V.-L. Yan, J.-B. Yan. Cold Regions Sci. Technol., **206** (4), 103751 (2022). DOI: 10.1016/j.coldregions.2022.103751
[46] D.M. Cole. Eng. Fract. Mech., **68**, 1797 (2001). DOI: 10.1016/S0013-7944(01)00031-5
[47] Yu. I. Golovin. Physics of the Solid State, **63** (1), 1 (2021). DOI: 10.1134/S1063783421010108
[48] W.H. Press, S.A. Teukolsky, W.T. Vetterling, B.P. Flannery. *Numerical Recipes in C: the art of Scientific Computing*, 2-nd ed. (Cambridge University Press, Cambridge, GB, 1992)

Translated by Ego Translating